Materials Science Forum Vols. 706-709 (2012) pp 1311-1317

doi:10.4028/www.scientific.net/MSF.706-709.1311

Non-isothermal Crystallization Kinetics of $Co_{67}Fe_4Cr_7Si_8B_{14}$ Amorphous Alloy

S.A. Hasheminezhad[1,a], M. Haddad-Sabzevar[2,b], S. Sahebian[3,c]

[1,2,3]Department of metallurgy and Materials Engineering, Engineering Faculty, Ferdowsi University of Mashhad, Box 91775-1111, Mashhad, Iran

[a]akram.hasheminezhad@gmail.com, [b]haddadm@ um.ac.ir, [c]samaneh.sahebian@gmail.com

Keywords: Co-based amorphous alloy, Thermal analysis, Non-isothermal crystallization kinetics.

Abstract. Non-isothermal crystallization kinetics of $Co_{67}Fe_4Cr_7Si_8B_{14}$ amorphous ribbons was studied by differential scanning calorimetry (DSC) technique under 10, 20, 30, 40 and 80 °Cmin^{-1} heating rates. It is found that $Co_{67}Fe_4Cr_7Si_8B_{14}$ amorphous alloy exhibits two-stage crystallization on heating. The two crystallization peaks shift to higher temperatures with increasing heating rate. The apparent activation energies (E_C) for the first stage of crystallization were determined as 443.44 and 434.47 kJmol^{-1} by using the Kissinger and Ozawa equations, respectively. Frequency factor (A) estimated to be 1.084×10^{26} s^{-1} using Kissinger equation. Kinetics parameters such as Crystallization exponent (n) and dimensionality of growth (N_{dim}) were determined using JMA (Johnson-Mehl-Avrami) method. Details of the nucleation and growth behaviours during the non-isothermal crystallization were studied in terms of local activation energy $E_C(x)$ by the OFW (Ozawa, Flynn and Wall) method. Also the activation energy for nucleation (E_n) and growth (E_g) separately estimated.

Introduction

Metallic amorphous alloys are known to possess unique physical, mechanical, magnetic and corrosion properties compared to conventional crystalline metals. These alloys are kinetically metastable. Most of them are stable at low temperatures and can crystallize at high temperatures [1], therefore thermal and thermodynamic characteristic during crystallization process changed [2]. Hence, the understanding of thermally-induced crystallization process in such systems is important from the application viewpoint.

The application of isothermal and non-isothermal experimental analysis techniques is most widely used for study of crystallization process in amorphous materials. Despite the isothermal techniques are decisive in most cases, the non-isothermal methods have several advantages over them. The non-isothermal experiments could be performed faster than isothermal experiments. These experiments could be used to extend the temperature range of measurements beyond that accessible to isothermal experiment. Since Practical processes occur under dynamic and non-isothermal conditions, the non-isothermal experiments have been suggested for the analysis of the DSC data [1, 3-5]. By Study of crystallization kinetics, the crystallization activation energy and crystallization exponent can be determined.

The aim of this work is studying the non-isothermal crystallization kinetics of $Co_{67}Fe_4Cr_7Si_8B_{14}$ amorphous alloy using DSC technique by Kissinger [6] and Ozawa [7] methods. In addition, the parameters of local activation energy and local Avrami exponent by OFW (Ozawa, Flynn and wall) method [8] are investigated.

Experimental procedure

$Co_{67}Fe_4Cr_7Si_8B_{14}$ alloy was prepared from pure materials and melted in a vacuum furnace. The planar flow melt spinning (PFMS) process was used for producing continuous ribbons [9]. The amorphous ribbons were 20 mm in width and 29±1 μm in thickness. The amorphous structure of the as-quenched ribbons was examined by X-ray diffraction (XRD, D8 Advance using Cu Kα radiation).

Thermal behavior of amorphous ribbons was investigated using a Shimadzu DSC60 differential scanning calorimeter (DSC). Calibration of the temperature scale was carried out by pure Indium standard (T_m = 156.6°C and ΔH_f = 28.5 Jg^{-1}) in every run to ensure accuracy and reliability of the data. The analyzed samples weighing about 1.6 mg were placed in aluminum pan, with an empty pan used as reference. Samples were examined from room temperature to 600 ºC by continuous heating at different heating rates of 10, 20, 30, 40 and 80 ºCmin^{-1}.

Results and Discussion

Non-isothermal crystallization behavior

The crystallization peaks of $Co_{67}Fe_4Cr_7Si_8B_{14}$ amorphous ribbons at 10, 20, 30, 40 and 80 ºC min^{-1} heating rates were illustrated in Figure 1. It is found that $Co_{67}Fe_4Cr_7Si_8B_{14}$ amorphous alloy exhibits two-stage crystallization on heating. In this work, the first crystallization peak was studied. The Crystallization onset temperature (T_x), peak temperature (T_p) and the enthalpy of first crystallization peak (ΔH_c) for whole DSC traces were listed in Table 1. With increasing the heating rate, the crystallization peaks shift to higher temperatures and become broader which indicate to a kinetic effect during crystallization which is normally found for crystallization in a nucleation-controlled region. Also by increasing heating rates, crystallization faster occurs (Figure 1b). At a low heating rate, there was sufficient time for nuclei with large enough size to become stable at a low temperature, thus the crystallization could begin at a low temperature [10].

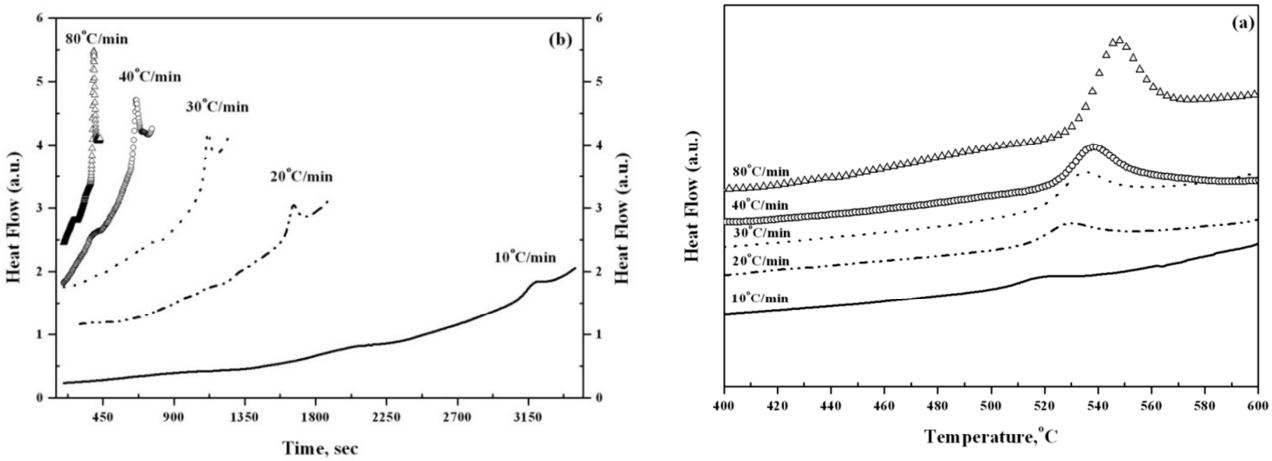

Fig. 1. Non-isothermal heating DSC curves against temperature (a) and time (b) for $Co_{67}Fe_4Cr_7Si_8B_{14}$ amorphous ribbons at different heating rates.

Table 1: The characteristic temperatures and crystallization enthalpy of $Co_{67}Fe_4Cr_7Si_8B_{14}$ amorphous ribbons at different heating rates

Heating rate, β[°Cmin^{-1}]	T_x [°C]	T_p [°C]	ΔH_c [jg^{-1}]
10	509.65	523.31	16.82
20	514.21	530.35	29.02
30	522.56	535.49	35.75
40	523.34	538.61	41.14
80	531.38	547.95	30.03

The curves shown in Figure 2 are the part of the DSC curves from 325°C to 510°C. Wide peak with low height that signed with arrow can be detected in all of curves. These peaks shift to higher temperature with increasing heating rate, indicated structural relaxation in amorphous alloy.

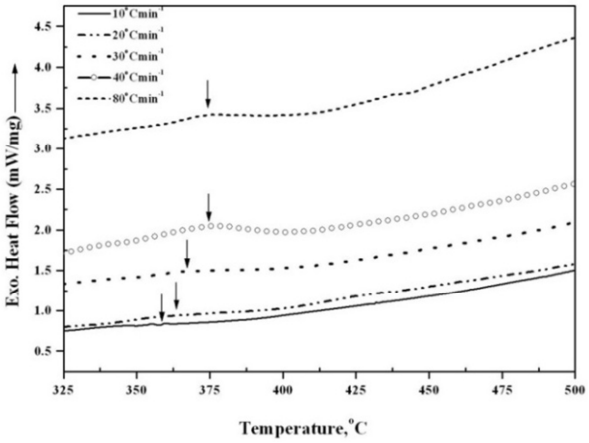

Fig. 2. DSC curves between 325°C to 500°C for $Co_{67}Fe_4Cr_7Si_8B_{14}$ amorphous ribbons at different heating rates.

The glass transition temperature (T_g) and crystallization temperature (T_x) in this alloy close together, therefore no distinct glass transition temperature was detected. Often the crystallization reaction starts in the temperature range where relaxation and glass transition take place, due to the high driving force resulting from the usually large undercooling. Therefore, for many amorphous alloys the relaxation and glass transition are covered by the onset of crystallization [11].

Non-isothermal Crystallization kinetics

Thermal behavior of metallic amorphous alloys during crystallization in isothermal conditions was described by a general equation for the reaction rate [12-14]:

$$\dot{x} = \frac{dx}{dt} = k(T)f(x). \quad (1)$$

Where f(x) is a function of the crystallized volume fraction (x), reflects the mechanism of crystallization, and k(T) is a reaction rate constant which is function of temperature.
According to Arrhenius's equation:

$$k(T) = A\exp\left(-\frac{E_c}{RT}\right). \quad (2)$$

Here A(s^{-1}) is the frequency factor and independent of temperature, E_c($kJmol^{-1}$) is the overall apparent activation energy for the crystallization process, R is the gas constant and T is the temperature. So the rate of conversion expressed by:

$$\dot{x} = \frac{dx}{dt} = A\exp(-\frac{E_c}{RT})\, f(x). \quad (3)$$

Under non-isothermal conditions with a constant heating rate of $\beta = \frac{dT}{dt}$, Eq. (3) was rewritten as:

$$\frac{dx}{dT} = \frac{A}{\beta}\exp\left(-\frac{E_c}{RT}\right)f(x). \quad (4)$$

Equation (4) by variables separation can be integrated:

$$\int_0^x \frac{dx}{f(x)} = \frac{A}{\beta}\int_0^{T_f}\exp\left(-\frac{E}{RT}\right)dT \approx \frac{AE}{\beta R}\int_{y_f}^{\infty}\frac{\exp(-y)}{y^2}\,dy. \quad (5)$$

β is heating rate, T_f the temperature at an equivalent (fixed) state of transformation, $y = \frac{E}{RT}$ and $y_f = \frac{E}{RT_f}$ .The integral on the right hand side in equation (5) is generally termed the temperature (p(y)) and does not have analytical solution.

$$P(y_f) = \int_{y_f}^{\infty} \frac{\exp(-y)}{y^2}\, dy. \quad (6)$$

To solve the temperature integral, several approximations were introduced. In general, all of these approximations lead to a direct isoconversion method in the form of:

$$\ln\left(\frac{\beta}{T_f^2}\right) = -\frac{E}{RT_f} + C. \quad (7)$$

C is an independent parameter of temperature and heating rate. To describe the process of crystallization, kinetics parameters such as activation energy (E_c), frequency factor (A) and crystallization exponent (n) should be determined.

By considering variation of peak temperature with heating rate (β), the overall apparent activation energy for the crystallization process can be estimated by Kissinger method [6]:

$$\ln\left(\frac{\beta}{T_p^2}\right) = -\frac{E_c}{RT_p} + \ln\left(\frac{AR}{E_c}\right). \quad (8)$$

Where T_p is peak crystallization temperature in DSC scan, β is the heating rate and R is a gas general constant. Figure 3 Shows the plot of $\ln(\beta/T_p^2)$ against $1000/T_p$ for different heating rates, which gives approximate straight line with slop of $(-E_c/R)$ and intercept of $\ln(AR/E_c)$. For the first crystallization stage, E_c and A were estimated about 443.44 kJmol^{-1} and 1.084×10^{26} s^{-1} from Kissinger method. The activation energy for $Co_{68}Fe_4Cr_4Si_{13}B_{11}$ amorphous alloy at heating rates ranging from 3 to 25 °Cmin^{-1} was reported 380 kJmol^{-1} [15].

In many cases, other equation is used to evaluate activation energy that called Ozawa equation:

$$\ln\beta = -1.0516\,\frac{E_c}{RT_p} + \text{const.} \quad (9)$$

Plot of lnβ against $1000/T_p$ yields straight line with slope of $(-1.0516E_C/R)$ (Figure 3). E_C is obtained 434.47 kJmol^{-1} from Ozawa method. These apparent activation energies show good agreement, indicating that the reaction order is close to unity [3].

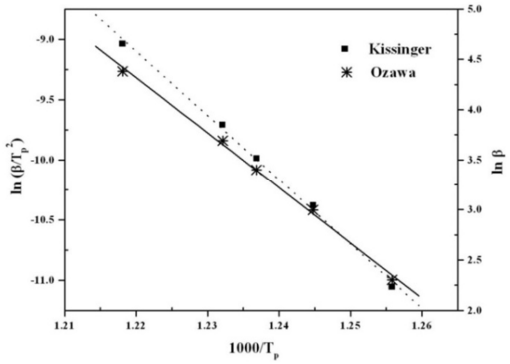

Fig. 3. $\ln(\beta/T_p^2)$ and lnβ against $1000/T_p$ for $Co_{67}Fe_4Cr_7Si_8B_{14}$ amorphous alloy.

The isothermal crystallization kinetics of amorphous alloy is normally analyzed by JMA equation to determine the mechanism of nucleation and growth [16]:

$$x = 1 - \exp\{-[k(t-\tau)]^n\}. \quad (10)$$

Where x is a crystallized volume fraction, k is the reaction rate constant which reflects both the rate of nucleation frequency and the crystal growth rate, τ is the incubation time and n is the Avrami exponent that reflects nucleation and growth mechanism. The values of n and k can be determined from the slop and intercept of plot of $\ln[-\ln(1-x)]$ vs. $\ln(t-\tau)$. This plot is shown in Figure 4. As shown in table 2, the crystallization exponent (n) is about 1.1 for this alloy.

According to values of the correlation parameter r for all of heating rates, can be deduced that JMA model is provided a satisfactory description to the non-isothermal crystallization of $Co_{67}Fe_4Cr_7Si_8B_{14}$ amorphous alloy.

Henderson has shown that the validity of the JMA equation can be extended in non-isothermal conditions if the entire nucleation process takes place during the early stages of the transformation, and it becomes negligible afterward [17-18]. Thus nucleation rate for this amorphous alloy is almost zero.

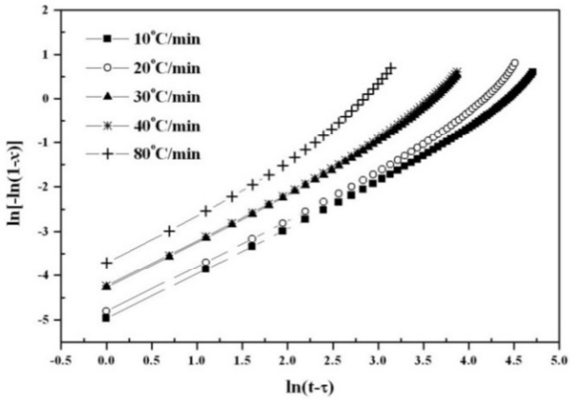

Fig. 4. Ln[-ln(1-x)] against ln(t-τ) by JMA equation for non-isothermal crystallization of $Co_{67}Fe_4Cr_7Si_8B_{14}$ amorphous alloy.

Table 2: Effect of heating rate on crystallization kinetics parameters

Heating rate, β[°Cmin^{-1}]	Avrami exponent [n]	reaction rate constant [k]	r
10	1.08	0.0092	0.9992
20	1.11	0.0117	0.9986
30	1.10	0.0193	0.9991
40	1.10	0.0199	0.9991
80	1.10	0.0337	0.9995

The crystallization exponent n can be expressed by the following equation [12, 15]:

$$n = N_{dim}g + B. \quad (11)$$

that N_{dim} is dimensionality of growth (with values 1, 2 and 3 for one, two and three dimensional growth, respectively), g is growth index (g=1 for interfaced controlled growth and g=0.5 for diffusion controlled growth) and B is nucleation index (B=0 in zero nucleation rate, B=1 for constant nucleation rate and B>1 for increasing nucleation rate).

For this amorphous alloy nucleation rate is almost zero (B=0), three dimensional growth is dominated and crystallization process controlled by diffusion of B and Si atoms.

Local activation energy

The apparent activation energy previously was calculated, usually gives the average value of crystallization activation energy. Therefore, local activation energy ($E_C(x)$) was defined that reflects the activation energy at any crystallized volume fraction (x). So the OFW (Ozawa, Flynn and Wall) method was applied:

$$\ln\beta = -1.0516\frac{E_c(x)}{RT_x} + \text{const.} \quad (12)$$

Where T_x is a temperature matching to fixed values of x from experiments at different heating rates. Plot of lnβ against $1000/T_x$ yields the approximately straight lines with slopes give ($-1.0516E_C(x)/R$) for a certain value of x. Thus can be depicted the plot of local activation energy, $E_C(x)$, against x for $Co_{67}Fe_4Cr_7Si_8B_{14}$ amorphous alloy (Figure 5). The average activation energy calculated by OFW is 371 kJmol^{-1}. This value is smaller than those acquired from Kissinger (443.44 kJ/mol) and Ozawa (434.47 kJ/mol) methods.

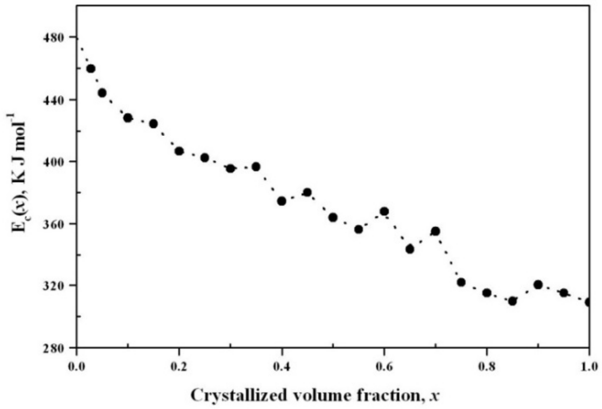

Fig. 5. Local activation energy against crystallized volume fraction by OFW method for $Co_{67}Fe_4Cr_7Si_8B_{14}$ amorphous alloy.

Activation energy for nucleation (E_n) and growth (E_g)

The activation energies for the nucleation and growth are related to the nucleation rate (I) and growth velocity (U) by the following equations:

$$I = I_0 \exp\left(-\frac{E_n}{RT}\right). \quad (13)$$

$$U = U_0 \exp\left(-\frac{E_g}{RT}\right).$$

Hence accurate measurement of these energies is necessary to understand the crystallization process and mechanism of nucleation and growth in amorphous alloys.

E_c value against volume crystallization fraction (x) was shown in Figure 5. In the early stage, the crystallization was ruled by nucleation, therefore U=0 and the activation energy $E_C(x=0) = E_n \simeq 479$ kJmol^{-1}. When the crystallization process continued, the crystallization mechanism was determined by both nucleation and growth, thus E_C is smaller than E_n but larger than E_g and decreased with increasing crystallized volume fraction (x). In the final stage, the crystallization was ruled by grain growth therefore I=0 and the activation energy $E_C(x=1) = E_g \simeq 309$ kJmol^{-1}.

Conclusion

1. The crystallization kinetics of $Co_{67}Fe_4Cr_7Si_8B_{14}$ amorphous ribbons was characterized by DSC under non-isothermal condition. The activation energy for crystallization of the amorphous alloy was calculated according to Kissinger and Ozawa methods, which gives E_C = 443.44 kJmol^{-1} for Kissinger and E_C = 434.47 kJmol^{-1} for Ozawa method. These activation energies have good consistency together.
2. Based on JMA equation, it was found that the crystallization mode of $Co_{67}Fe_4Cr_7Si_8B_{14}$ amorphous alloys is governed by nucleation rate near to zero and three-dimensional diffusion controlled growth.
3. The average activation energy derived from OFW method is 371kJmol^{-1} and lower than Kissinger and Ozawa equations.
4. The values of E_n and E_g in a $Co_{67}Fe_4Cr_7Si_8B_{14}$ amorphous alloy was obtained using plot of $E_C(x)$ against x. The values of E_n and E_g is 479 kJmol^{-1}and 309 kJmol^{-1}, respectively.

References

[1] T.L. Shanker Rao, K.N. Lad and A.Pratap: J. Therm. Anal. Vol. 78 (2004), p. 769.
[2] H.F. Li and R.V. Ramanujan: Mater. Sci. A 375–377 (2004), p. 1087.
[3] Z.Z. Yuan, X.D. Chen, B.X. Wang and Y.J. Wang: J. Alloys Compd. Vol. 407 (2006), p. 163.
[4] K. Song, X. Bian, J. Guo, X. Li, M. Xie and C. Dong: J. Alloys Compd. Vol. 465 (2008), p. L7.
[5] J. Vázquez, P.L. López-Alemany, P. Villares and R. Jiménez-Garay: Mater. Chem. Vol. 57 (1998), p. 162.

[6] H.E. Kissinger: Anal. Chem. Vol. 29 (1957), p. 1702.
[7] T.Ozawa: Bull. Chem. Soc. Jpn. Vol. 38 (1965), p.1881.
[8] T.Ozawa: J. Thermal Anal. Vol. 2 (1970), p. 301.
[9] M. Haddad-Sabzevar: Ph. D. Thesis. *Ribbon formation and solidification behavior in planar flow melt spinning process*. Stockholm (1994).
[10] P. Supaphol, P. Thanomkiat, J. Junkasem and R. Dangtungee: Polym. Test. Vol. 26 (2007), p. 20.
[11] H. Nitsche, M. Stanislowski, F. Sommer and E.J. Mittemeijer: Ph. D. Thesis. *Kinetics of crystallization in amorphous alloys; nucleation and growth.* Universität Stuttgart (2005).
[12] D.M. Minić, A. Maričić and B. Adnadević: J. Alloys Compd. Vol. 473 (2009), p. 363.
[13] A.A. Joraid, A.A. Abu-sehly, M. Abu El-Oyoun and S.N. Alamri: Thermochim. Acta. Vol. 470 (2008), p. 98.
[14] M.J. Starink: Thermochim. Acta. Vol. 404 (2003), p. 163.
[15] I.C. Rho, C.S. Yoon, C.K. Kim, T.Y. Byun and K.S. Hong: Mater. Sci. B 96 (2002), p. 48.
[16] J.S.C. Jang, I.H. Wang, L.J. Chang, G.J. Chen, T.H. Hung and J.C. Huang: Mater. Sci. A. 449–451 (2007), p. 511.
[17] D.W. Henderson: Therm. Anal. Vol. 15 (1979), p. 325.
[18] D.W. Henderson: J. Non-Cryst. Solids. Vol. 30 (1979), p. 301.